APPLIED AND ENVIRONMENTAL MICROBIOLOGY, Sept. 2010, p. 6047–6055 Vol. 76, No. 18
0099-2240/10/$12.00 doi:10.1128/AEM.00742-10

Transcriptional Regulation of the Terephthalate Catabolism Operon in *Comamonas* sp. Strain E6[▽]

Daisuke Kasai, Masahiro Kitajima, Masao Fukuda, and Eiji Masai*

Department of Bioengineering, Nagaoka University of Technology, Nagaoka, Niigata 940-2188, Japan

Received 24 March 2010/Accepted 12 July 2010

Two almost identical gene clusters, $tphR_IC_IA2_IA3_IB_IA1_I$ and $tphR_{II}C_{II}A2_{II}A3_{II}B_{II}A1_{II}$, are responsible for the conversion of terephthalate (TPA) to protocatechuate in *Comamonas* sp. strain E6. In the present study, we investigated the transcriptional regulation of the $tphR_{II}C_{II}A2_{II}A3_{II}B_{II}A1_{II}$ gene cluster. Reverse transcription-PCR analysis suggested that the $tphR_{II}C_{II}A2_{II}A3_{II}B_{II}A1_{II}$ genes form two transcriptional units, the $tphC_{II}A2_{II}A3_{II}B_{II}A1_{II}$ catabolism operon and $tphR_{II}$, with the latter encoding an IclR-type transcriptional regulator (ITTR). The transcription start site of the tph_{II} catabolism operon was mapped at 21 nucleotides upstream of the initiation codon of $tphC_{II}$. The *lacZ* transcriptional fusion experiments showed that $tphR_{II}$ encodes a transcriptional activator of the tph_{II} catabolism operon and that TPA acts as an inducer. On the other hand, $TphR_{II}$ appeared to repress its own transcription regardless of the presence of TPA. The analysis of mutant derivatives of E6 indicated that $tphR_{II}$ is essential for the transcriptional activation of the tph_{II} catabolism operon and the growth on TPA of a tph_I-deficient derivative of E6. Purified His-tagged $TphR_{II}$ bound specifically to the $tphR_{II}$-$tphC_{II}$ intergenic region containing a 21-bp inverted repeat sequence. Alignment of the inverted repeat sequences in the binding sites for $TphR_{II}$ and other members of ITTRs revealed highly conserved nucleotides. The substitution of conserved nucleotides resulted in significantly reduced TPA-dependent transcriptional activation from the $tphC_{II}$ promoter and reduced binding to His-tagged $TphR_{II}$. These results clearly indicate that the conserved nucleotides are required for the inducible expression of the tph_{II} catabolism operon regulated by $TphR_{II}$.

The phthalate isomers terephthalate (TPA), isophthalate, and *o*-phthalate are widely used as plasticizers and are degraded by microbial catabolic pathways via protocatechuate (PCA) (8, 9, 26, 30). The degradation of PCA is catalyzed by one of the following three aromatic ring cleavage pathways: the PCA 2,3-cleavage (17), the PCA 3,4-cleavage (14), or the PCA 4,5-cleavage (19, 20) pathway. 2-Pyrone-4,6-dicarboxylate (PDC), which appears as an intermediate metabolite in the PCA 4,5-cleavage pathway (19, 20), has been considered to be a useful chemical building block for the synthesis of biodegradable and high-function polymers (15, 22, 23). Due to the potentiality of phthalate isomers to act as starting materials for the production of PDC, it has become increasingly more important to elucidate the microbial catabolism genes for phthalates and their regulation.

Previously, our research group isolated a TPA degrader, *Comamonas* sp. strain E6, which is able to grow on TPA, isophthalate, and *o*-phthalate as the sole source of carbon and energy; and these compounds are degraded via the PCA 4,5-cleavage pathway (9, 30). We reported on the characterization of two almost identical TPA catabolism gene clusters (>94% identity) of E6, $tphR_IC_IA2_IA3_IB_IA1_I$ (GenBank accession no. AB238678) and $tphR_{II}C_{II}A2_{II}A3_{II}B_{II}A1_{II}$ (GenBank accession no. AB238679) (30). The catabolism of TPA is initiated by the transformation of TPA into 1,2-dihydroxy-3,5-cyclohexadiene-1,4-dicarboxylate (1,4-DCD) by TPA 1,2-dioxygenase (oxygenase component, TphA2 and TphA3; reductase component, TphA1), and 1,4-DCD is converted to PCA by 1,4-DCD dehydrogenase (TphB) (Fig. 1A). The resulting PCA is further degraded via the PCA 4,5-cleavage pathway. On the basis of the amino acid sequence similarity and the findings of expression studies, *tphC* and *tphR* were suggested to code for a receptor and a regulator involved in TPA catabolism: a periplasmic TPA binding receptor and an IclR-type transcriptional regulator (ITTR), respectively.

The TPA catabolic pathway has also been reported in *Comamonas testosteroni* T-2 (32), *C. testosteroni* YZW-D (37), *Delftia tsuruhatensis* T7 (33), *Rhodococcus* sp. strain DK17 (4), and *Rhodococcus jostii* RHA1 (13). The TPA catabolism gene clusters were identified in YZW-D, DK17, and RHA1; and all of these gene clusters include a gene encoding a putative ITTR, which appeared to be involved in TPA catabolism. Several ITTRs involved in the degradation of aromatic compounds have been described. This family includes, among others, PcaU and PcaR, activators of β-ketoadipate pathway genes in *Acinetobacter baylyi* ADP1 (5, 10) and *Pseudomonas putida* PRS2000 (29), respectively; PobR, an activator of the *p*-hydroxybenzoate 3-hydroxylase gene, *pobA*, from *A. baylyi* ADP1 (6); as well as CatR, a repressor of the catechol *ortho*-cleavage pathway genes in *Rhodococcus erythropolis* CCM2595 (36). However, the transcriptional regulation of TPA catabolism genes has not yet been reported.

In this report, we describe the transcriptional control of one of the *tph* catabolism gene clusters, $tphC_{II}A2_{II}A3_{II}B_{II}A1_{II}$, regulated by the $tphR_{II}$ gene product. This is the first report on the characterization of the regulation of TPA catabolism genes.

* Corresponding author. Mailing address: Department of Bioengineering, Nagaoka University of Technology, Nagaoka, Niigata 940-2188, Japan. Phone and fax: 81-258-47-9428. E-mail: emasai@vos.nagaokaut.ac.jp.

▽ Published ahead of print on 23 July 2010.

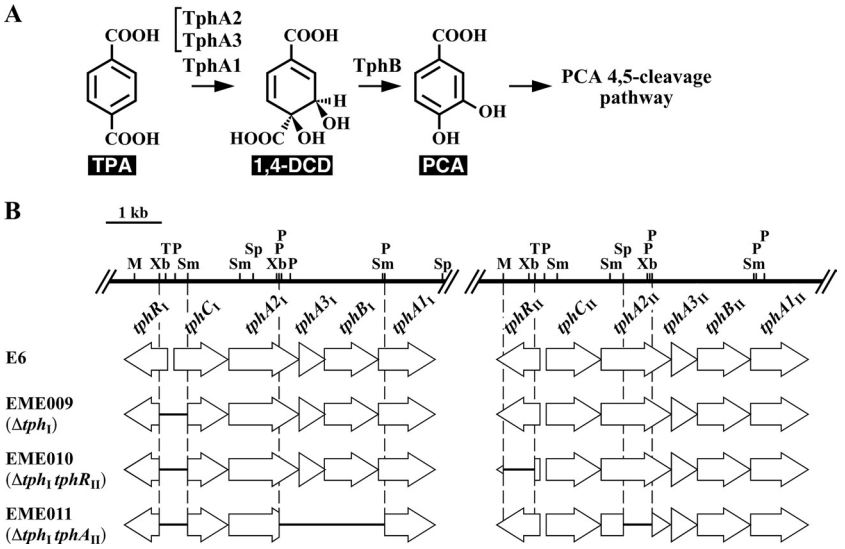

FIG. 1. TPA catabolic pathway of *Comamonas* sp. strain E6 (A) and schematic diagrams of the gene disruptions in E6 (B). (A) TphA2, oxygenase large subunit of TPA 1,2-dioxygenase; TphA3, oxygenase small subunit of TPA 1,2-dioxygenase; TphA1, reductase component of TPA 1,2-dioxygenase; TphB, 1,4-DCD dehydrogenase. (B) The horizontal bars in the thick arrows indicate the regions deleted in EME009, EME010, and EME011. Abbreviations for restriction enzymes: M, MunI; P, PstI; Sm, SmaI; Sp, SphI; T, Tth111I; Xb, XbaI.

MATERIALS AND METHODS

Bacterial strains, plasmids, and culture conditions. The bacterial strains and plasmids used in this study are listed in Table 1. *Comamonas* sp. strain E6 was grown in Luria-Bertani (LB) medium or in W minimal salt medium (27) containing 10 mM TPA or 10 mM succinate at 30°C. *Escherichia coli* strains were grown in LB medium at 37°C. For cultures of cells carrying antibiotic resistance markers, the media for *E. coli* transformants were supplemented with 100 mg of ampicillin (Ap)/liter or 25 mg of kanamycin (Km)/liter, and the media for E6 transformants were supplemented with 50 mg of Km/liter or 30 mg of chloramphenicol/liter.

DNA manipulations and nucleotide sequencing. DNA manipulations, including total DNA isolation, construction of deletion derivatives, and nucleotide sequencing, were performed as described previously (18). Analysis of nucleotide sequences was carried out as described previously (1).

Generation of mutants. The 2.5-kb EcoRV-HindIII fragment carrying *tphR*$_I$ and *tphC*$_I$ of pSS92R was inserted into pK19*mobsacB* to generate pK19RCI. The 0.5-kb XbaI-SmaI fragment including the intergenic region between *tphR*$_I$ and *tphC*$_I$ of pK19RCI was deleted. The resulting plasmid, pDTRCI, was introduced into E6 cells by electroporation, and candidates for the deletion mutant of the *tphR*$_I$-*tphC*$_I$ intergenic region (strain EME009) were isolated (Fig. 1B) as described previously (21). In order to disrupt the *tphR*$_{II}$ gene in EME009, the 0.6-kb MunI-Tth111I fragment of the *tphR*$_{II}$ internal region in pEJ89 was deleted, and then the 2.3-kb EcoRI-HindIII fragment carrying part of *tphR*$_{II}$ was cloned into pK19*mobsacB.* The resulting plasmid, pDTRII, was further introduced into EME009 cells, and candidates for the mutant (strain EME010) were isolated (Fig. 1B). To obtain a mutant which lacked the ability to transform TPA, the *tphA2*$_{II}$ disruption plasmid, pDTA2II, was introduced into EME009 cells. Furthermore, the *tphA2*$_I$*A3*$_I$*B*$_I$*A1*$_I$ disruption plasmid, pDTABI, was introduced into the resulting mutant cells to obtain EME011 (Fig. 1B).

Disruption of the genes was examined by Southern hybridization analysis. To confirm the disruptions of the *tphR*$_I$-*tphC*$_I$ intergenic region, *tphR*$_{II}$, and *tphA2*$_{II}$, total DNA of candidates for mutants were digested with HincII-HindIII. To confirm the *tphA2*$_I$*A3*$_I$*B*$_I$*A1*$_I$ deletion, total DNA of candidates for the mutant was digested with HindIII. The 0.8-kb XbaI-PvuII fragment carrying the *tphR*$_I$-*tphC*$_I$ intergenic region, the 1.3-kb PstI fragment carrying *tphR*$_{II}$, and the 0.9-kb SmaI-NcoI fragment carrying *tphA2*$_{II}$ were labeled with a digoxigenin (DIG) system (Roche, Mannheim, Germany) and used as probes.

Reverse transcription (RT)-PCR. EME009 cells were grown in W minimal salt medium supplemented with 10 mM TPA or 10 mM succinate at 30°C. When the absorbance at 600 nm (A_{600}) of the culture was 1.0, the cells were harvested by centrifugation at 5,000 × *g* at 4°C for 10 min. Total RNA was isolated with the Isogen reagent (Nippon Gene, Toyama, Japan), according to the manufacturer's instructions. Purified RNA was then treated with RNase-free DNase I (Takara Bio Inc., Otsu, Japan) to remove contaminating DNA. Single-stranded cDNA was synthesized from 5.0 μg of total RNA utilizing PrimeScript reverse transcriptase (Takara Bio Inc.) with random primers in a 20-μl reaction mixture. PCR amplification was performed using 2.0 μl of the cDNA mixture, specific primers (Table 2), and Ex *Taq* DNA polymerase (Takara Bio Inc.) under the following conditions: 95°C for 30 s and 35 cycles of 95°C for 60 s, 62°C for 60 s, and 72°C for 60 s. A control without reverse transcriptase was used for each reaction to verify the absence of genomic DNA contamination. Samples from the PCR were electrophoresed on a 1.8% agarose gel and visualized with ethidium bromide.

Primer extension. E6 cells harboring pKTtphII were grown in W minimal salt medium containing 10 mM succinate either with or without 10 mM TPA at 30°C. After 4 h of incubation, total RNA was isolated as described above. The primers used to detect the start sites of *tphC*$_{II}$ and *tphR*$_{II}$ mRNAs were PEtphC110 and PEtphR160 (Table 2), respectively, which are complementary to the nucleotide sequences between positions +90 and +110 and between positions +138 and +157 relative to the start codons of *tphC*$_{II}$ and *tphR*$_{II}$, respectively. The primers were labeled at their 5′ ends with dye D4 (Beckman Coulter Inc., Fullerton, CA). A labeled primer (2 pmol) was hybridized to 5.0 μg of the total RNA preparation. A primer extension reaction was performed by incubating the annealing mixture with 200 U of PrimeScript reverse transcriptase at 42°C for 45 min. After the extension, the enzyme was inactivated by being exposed to a temperature of 95°C for a period of 10 min and ethanol precipitated. The products were then analyzed by a CEQ2000XL genetic analysis system (Beckman Coulter Inc.).

LacZ transcriptional fusions and β-galactosidase activity assays. To determine the promoter activities of *tphC*$_{II}$ and *tphR*$_{II}$, pZTC and pZTR, which expressed the *tphC*$_{II}$ promoter-*lacZ* fusion and the *tphR*$_{II}$ promoter-*lacZ* fusion, respectively, were introduced into cells of E6 and its mutant derivatives by electroporation. The resulting transformants were grown in W minimal salt medium containing 10 mM succinate either with or without 10 mM TPA, phthalate, isophthalate, or PCA at 30°C. After 4 h of incubation, cells were harvested and resuspended in 20 mM Tris-HCl buffer (pH 8.0), broken by an ultrasonic disintegrator (UD-201; Tomy Seiko Co., Tokyo, Japan), and centrifuged at 15,000 × *g* for 15 min. The resulting supernatants were used as crude enzymes. The protein concentration was determined by the Bradford method (3).

β-Galactosidase activity assays with 4-methylumbelliferyl-β-D-galactopyranoside (4MUG) as the substrate were performed as follows. A 300-μl assay mixture contained 20 mM Tris-HCl (pH 8.0), crude extract (50 μg or 1 mg of protein), and 300 μM 4MUG. After incubation of said mixture for 15 min, 200 μl of the reaction mixture was transferred to 1.8 ml of 100 mM glycine-NaOH buffer (pH 10.0), and then the production of 4-methylumbelliferone (4MU) was detected with an RF-1500 spectrofluorometer (Shimadzu, Kyoto, Japan). One unit of enzyme activity was defined as the amount of enzyme that resulted in the

TABLE 1. Strains and plasmids used in this study

Strain or plasmid	Relevant characteristic(s)[a]	Source or reference
Comamonas sp.		
E6	Wild type, TPA^+	30
EME009	E6 derivative, Δ$tphR_I$ $tphC_I$	This study
EME010	EME009 derivative, Δ$tphR_{II}$	This study
EME011	EME009 derivative, Δ$tphA2_IA3_IB_IA1_I$ $tphA2_{II}$	This study
E. coli		
DH5α	*supE44* Δ*lacU169* (ϕ80 *lacZ*ΔM15) *hsdR17 recA1 endA1 gyrA96 thi-1 relA1*	12
XL2-Blue	*recA1 endA1 gyrA96 thi-1 hsdR17 supE44 relA1 lac* [F′ *proAB lacI*^{q}ZΔM15 Tn*10* (Tc^r) Amy Cm^r]	Stratagene
BL21(DE3)	F^- *ompT* $hsdS_B(r_B^-\ m_B^-)$ *gal dcm* (DE3), T7 RNA polymerase gene under control of the *lacUV* promoter	35
Plasmids		
pBluescript II SK(+)	Cloning vector, Ap^r	34
pT7Blue	Cloning vector, Ap^r T7 promoter	Novagen
pK19*mobsacB*	*oriT sacB* Km^r	31
pKT230MC	IncQ broad-host-range cloning vector, Km^r	25
pJB866	RK2 broad-host-range expression vector, Tc^r P_m *xylS*	2
pET16b	Expression vector, N-terminal His_{10} tag, Ap^r T7 promoter	Novagen
pPR9TZ	Broad-host-range promoter probe vector, RK2 *ori* Ap^r Cm^r	17
pSS92R	pBluescript II SK(+) with a 4.0-kb SalI fragment carrying $tphR_I$ and $tphC_I$	This study
pK19RCI	pK19*mobsacB* with a 2.5-kb EcoRV-HindIII fragment of pSS92R	This study
pDTRCI	pK19RCI with a deletion of a 0.5-kb XbaI-SmaI fragment carrying the $tphR_I$-$tphC_I$ intergenic region	This study
pEJ89	pJB866 with a 8.9-kb EcoRI fragment carrying $tphR_IIC_IIA2_IIA3_IIB_IIA1_II$	30
pEJ84	pEJ89 with a deletion of a 0.6-kb MunI-Tth111I fragment carrying part of $tphR_{II}$	30
pDTRII	pK19*mobsacB* with a 2.3-kb EcoRI-HindIII fragment of pEJ84	This study
pK19A2II	pK19*mobsacB* with a 2.0-kb HindIII-XhoI fragment carrying $tphA2_{II}$	This study
pDTA2II	pK19A2II with a deletion of a 0.5-kb SphI-PstI fragment carrying part of $tphA2_{II}$	This study
pK19ABIF	pK19*mobsacB* with a 4.3-kb HindIII fragment carrying $tphA2_IA3_IB_IA1_I$	This study
pDTABI	pK19ABIF with a deletion of a 1.9-kb PstI fragment carrying $tphA2_IA3_IB_IA1_I$	This study
pKTRII	pKT230MC with a 1.8-kb KpnI fragment carrying $tphR_{II}$	This study
pKTtphII	pKT230MC with a 8.9-kb EcoRI fragment carrying $tphR_IIC_IIA2_IIA3_IIB_IIA1_II$	This study
pTRII	pT7Blue with a 779-bp PCR fragment generated by the TphRII-F and TphRII-R primer pair	This study
pETtprII	pET16b with a 772-bp NdeI-XhoI fragment of pTRII	This study
pTTC	pT7Blue with a 393-bp PCR fragment carrying the $tphR_{II}$-$tphC_{II}$ intergenic region	This study
pZTC	pPR9TZ with a 381-bp HindIII-KpnI fragment of pTTC	This study
pTTR	pT7Blue with a 500-bp PCR fragment carrying the $tphR_{II}$-$tphC_{II}$ intergenic region	This study
pZTR	pPR9TZ with a 379-bp HindIII-KpnI fragment of pTTR	This study
pTTCT5C	Site-directed mutant of pTTC generated by the SMT5C-F and SMT5C-R primer pair	This study
pTTCG6A	Site-directed mutant of pTTC generated by the RM315-F and RM315-R primer pair	This study
pTTCC7T	Site-directed mutant of pTTC generated by the SMC7T-F and SMC7T-R primer pair	This study
pTTCG8A	Site-directed mutant of pTTC generated by the SMG8A-F and SMG8A-R primer pair	This study
pT5C	pPR9TZ with a 381-bp HindIII-KpnI fragment of pTTCT5C	This study
pG6A	pPR9TZ with a 381-bp HindIII-KpnI fragment of pTTCG6A	This study
pC7T	pPR9TZ with a 381-bp HindIII-KpnI fragment of pTTCC7T	This study
pG8A	pPR9TZ with a 381-bp HindIII-KpnI fragment of pTTCG8A	This study

[a] Abbreviations: TPA^+, able to grow on TPA as the sole carbon source; Ap^r, Km^r, Tc^r, and Cm^r, resistance to ampicillin, kanamycin, tetracycline, and chloramphenicol, respectively.

production of 1 μmol of 4MU per min. Specific activity was expressed in units per milligram of protein.

Expression of His tag-fused $tphR_{II}$ in *E. coli*. The coding region of $tphR_{II}$ was amplified by PCR using Ex *Taq* DNA polymerase together with pKTtphII as the template as well as the TphRII-F and TphRII-R primer pair (Table 2). The 779-bp PCR product was cloned in pT7Blue and sequenced. The 772-bp NdeI-XhoI fragment of the resulting plasmid was inserted into pET16b to generate pETtprII, which fused the codons for 10 histidines (His tag) at the 5′ end of $tphR_{II}$. *E. coli* BL21(DE3) cells harboring pETtprII were grown in 1 liter of LB medium containing 100 mg of Ap/liter at 30°C. When the A_{600} of the culture reached 0.5, the expression of His tag-fused $tphR_{II}$ was induced for 2 h by adding 1 mM isopropyl-β-D-thiogalactopyranoside. After the incubation, cells were harvested and resuspended in 50 mM Tris-HCl buffer (pH 7.5), broken by three passages through a French pressure cell (Aminco, Urbana, IL), and centrifuged at 26,000 × *g* for 20 min. The resulting supernatants were used as crude enzymes.

Purification of His-$TphR_{II}$. To remove nucleic acids, streptomycin sulfate was added to the crude enzyme to a final concentration of 1%. The lysate was kept on ice for 10 min and centrifuged at 15,000 × *g* for 15 min. The supernatant was applied to an Ni Sepharose 6 Fast Flow column (GE Healthcare, Buckinghamshire, United Kingdom) previously equilibrated with buffer A, consisting of 50 mM Tris-HCl (pH 7.5), 500 mM NaCl, and 40 mM imidazole. Proteins were allowed to bind for 1 min at 4°C while they were rotated, followed by washing five times in 5 ml of buffer B, consisting of 50 mM Tris-HCl (pH 7.5), 500 mM NaCl, and 100 mM imidazole. His-tagged $TphR_{II}$ (His-$TphR_{II}$) was eluted with 5 ml of buffer C, consisting of 50 mM Tris-HCl (pH 7.5), 500 mM NaCl, and 500 mM imidazole; and 500-μl fractions were pooled and concentrated by centrifugal filtration with a Microcon YM-30 apparatus (Millipore, Billerica, MA). The purity of the enzyme preparation was examined by sodium dodecyl sulfate–12% polyacrylamide gel electrophoresis (SDS-PAGE).

Electrophoretic mobility shift assays (EMSAs). DNA fragments containing the $tphR_{II}$-$tphC_{II}$ intergenic region were synthesized by PCR with the specific primer pairs (Table 2). To prepare the RM31 and G6A probes, the RM31-F and RM31-R and the RM315-F and RM315-R oligonucleotide pairs, respectively, were annealed to each other. To prepare probes T5C, C7T, and G8A, the DNA

TABLE 2. Primer sequences used in this study

Primer use and primer	Sequence (5′–3′)[a]
RT-PCR analysis	
insxRF	CCTAACAGCAATGCTCATGG
insRR	ACTACTGGATGCACTGTCGG
intRCF	ACAGTGCATCCAGTAGTGGC
intRCR	AGGCTAGCACAGTCATTCCG
insCF	ACGGAATGACTGTGCTAGCC
insCR	GGATGAACTGAGCAGTCTTGG
intCA2F	CGAGAAGTGGAAGAAGGTGC
intCA2R	TTGTGAGAGGCGATTCAGC
intA2A3F	GCTGCCTAACAACTGGAAGC
intA2A3R	GCAATAGTGGCAATCCTTGG
intA3BF	TGTCGACAACCATGATGAGG
intA3BR	ACGATGTCTTGAAGAAGCGG
intBA1F	ACGACCTGTATGTAGCCATGC
intBA1R	ATAGTGCTGAAGCGACCACC
insA1F	GATCCATATCCACGACTCCG
insA1R	ATGGCGCTAGGAAGATACAGG
Primer extension	
PEtphC110	GGCACGACGATCTTGAGAGG
PEtphR160	GCTGTACCAGTGTGCTGAGC
Construction of promoter-*lacZ* fusion plasmids	
HRC-F	AAGCTTGAGCGAACGTCTGG (HindIII)
HRC-R	GGAACACTAGATCGGCACC
KRCH-F	GGTACCGATAGCCAAGCTGTACC (KpnI)
KRCH-R	AAGCTTCGACGATCTTGAGAGG (HindIII)
Construction of $tphR_{II}$ expression plasmids	
TphRII-F	CATATGCAGGACAAGAACTTTGTGG (NdeI)
TphRII-R	CTCGAGCACTACAACCCCTGCG (XhoI)
EMSAs	
RMF01	GTTCTTGTCCTGCATAGCG
RMF11	GACATCCTCATACTGCAGTTCC
RMR01	GTCTGCGAATAGATTCGTTGC
RMR11	AACTGCAGTATGAGGATGTCG
RM31-F	CAACATTTTTGCGCATAGCGCAAAAACAGGT
RM31-R	ACCTGTTTTTGCGCTATGCGCAAAAATGTTG
RM315-F	CAACATTTTTaCGCATAGCGCAAAAACAGGT
RM315-R	ACCTGTTTTTGCGCTATGCGtAAAAATGTTG
Site-directed mutagenesis	
SMT5C-F	GGTGTTTTCAACATTTTcGCGCATAGCGCAAAAACAGG
SMT5C-R	CCTGTTTTTGCGCTATGCGCgAAAATGTTGAAAACACC
SMC7T-F	GGTGTTTTCAACATTTTTGtGCATAGCGCAAAAACAGG
SMC7T-R	CCTGTTTTTGCGCTATGCaCAAAAATGTTGAAAACACC
SMG8A-F	GGTGTTTTCAACATTTTTGCaCATAGCGCAAAAACAGG
SMG8A-R	CCTGTTTTTGCGCTATGtGCAAAAATGTTGAAAACACC

[a] Engineered restriction sites are underlined, and the corresponding restriction enzymes are shown in parentheses. Mutated nucleotides are in lowercase.

fragments were amplified from pTTCT5C, pTTCC7T, and pTTCG8A, respectively, using the RMF01 and RMR01 primer pair. The 3′ ends of the fragments of probes were labeled with DIG-11-ddUTP utilizing the 2nd-generation DIG gel shift kit (Roche), according to the manufacturer's instructions. Binding reactions were performed in 10-μl reaction mixtures containing 20 ng of purified His-TphR_{II} (65 nM monomer), 0.1 or 1 nM DIG-labeled probes, 1 μg of poly[d(I-C)], 0.1 μg of poly-L-lysine, and 1× reaction buffer (20 mM Tris-HCl [pH 8.0], 100 mM KCl, 10% glycerol, 5 mM EDTA). The mixtures were then incubated at 20°C for 20 min, loaded onto 10% polyacrylamide gels in 0.5× Tris-borate-EDTA buffer, and then separated by gel electrophoresis at 80 V for 120 to 150 min. Subsequently, the DIG-labeled DNA was transferred to a nylon membrane (Hybond-N; GE Healthcare) at 200 mA for 1 h with a Trans Blot SD apparatus (Bio-Rad, Hercules, CA) and then visualized by an enzyme immunoassay using a DIG gel shift kit, following the manufacturer's instructions. For detection of the labeled DNA, X-ray film was used. In competitive assays, a 1,000-fold molar excess of unlabeled probe was added to the preformed protein-DNA complexes.

Site-directed mutagenesis of the $tphR_{II}$-$tphC_{II}$ intergenic region. Site-directed substitutions in the inverted repeat sequence occurring in the $tphR_{II}$-$tphC_{II}$ intergenic region were introduced using a QuikChange site-directed mutagenesis kit (Stratagene, San Diego, CA) and plasmid pTTC as the template, according to the manufacturer's instructions. The oligonucleotides used for site-directed mutagenesis are listed in Table 2. All mutational changes were verified by DNA sequencing.

RESULTS AND DISCUSSION

RT-PCR analysis of tph_{II} genes. Because tph_I and tph_{II} gene clusters are organized as *tphR* and *tphCA2A3BA1*, which are divergently transcribed from one another, the promoter regions for *tphR* and *tphC* were expected to be present in the *tphR-tphC* intergenic regions. Due to the fact that the nucleo-

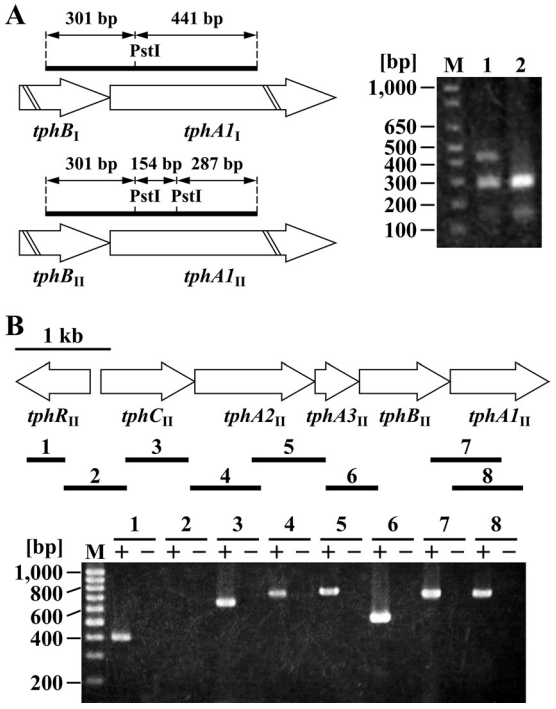

FIG. 2. RT-PCR analysis of the *tph* gene clusters. (A) Agarose gel electrophoresis of the RT-PCR products digested with PstI. RT-PCR was performed using total RNAs extracted from the cells of E6 and EME009 grown on TPA and the intBA1F and intBA1R primer pair. Lane M, molecular size markers; lanes 1 and 2, PstI digests of RT-PCR products obtained from E6 and EME009 cells, respectively. (B) Total RNA used for cDNA synthesis was isolated from EME009 cells grown on TPA. The results of agarose gel electrophoresis of the products of RT-PCR assays with primers targeting $tphR_{II}$ (lane 1; expected size, 403 bp), $tphR_{II}$-$tphC_{II}$ (lane 2; expected size, 666 bp), $tphC_{II}$ (lane 3; expected size, 657 bp), $tphC_{II}$-$tphA2_{II}$ (lane 4; expected size, 745 bp), $tphA2_{II}$-$tphA3_{II}$ (lane 5; expected size, 771 bp), $tphA3_{II}$-$tphB_{II}$ (lane 6; expected size, 533 bp), $tphB_{II}$-$tphA1_{II}$ (lane 7; expected size, 742 bp), and $tphA1_{II}$ (lane 8; expected size, 738 bp) are shown. Lane M, molecular size markers; lanes + and −, RT-PCR with and without reverse transcriptase, respectively.

tide sequences of the $tphR_I$-$tphC_I$ and $tphR_{II}$-$tphC_{II}$ intergenic regions (109 bp) are identical and the amino acid sequence identity between $TphR_I$ and $TphR_{II}$ is 99%, the transcriptional regulation of both operons was thought to be the same. For all of these reasons, we focused on the regulation of the tph_{II} gene cluster. In order to characterize the transcription of the tph_{II} genes, we constructed a mutant of *Comamonas* sp. strain E6, EME009, in which the $tphR_I$-$tphC_I$ intergenic region was deleted (Fig. 1B). To verify the effect of the deletion of the $tphR_I$-$tphC_I$ intergenic region on E6 cells, RT-PCR was performed using total RNAs extracted from the cells of E6 and EME009 and the intBA1F and intBA1R primer pair, which was designed to amplify a 742-bp region of the tph_I and tph_{II} gene clusters (Fig. 2A). The resulting RT-PCR products were digested with PstI and then analyzed by agarose gel electrophoresis. In the case of the wild-type strain, fragments of 301 bp and 441 bp derived from tph_I and fragments of 301 bp, 287 bp, and 154 bp derived from tph_{II} were observed. However, the 441-bp fragment was missing in the digested fragments obtained from EME009 cells, indicating that the tph_I genes were no longer transcribed in EME009 cells (Fig. 2A). The growth rate of EME009 cells on TPA was almost identical to that of the wild-type strain (data not shown). This result indicates that the tph_{II} gene cluster is sufficient to support the normal growth of E6 on TPA.

RT-PCR experiments were performed with total RNA extracted from EME009 cells grown on TPA and primers complementary to neighboring tph_{II} genes, as shown in Fig. 2B. RT-PCR products of the expected sizes were detected for the internal regions of $tphR_{II}$, $tphC_{II}$, and $tphA1_{II}$ and the intergenic regions of $tphC_{II}$-$tphA2_{II}$, $tphA2_{II}$-$tphA3_{II}$, $tphA3_{II}$-$tphB_{II}$, and $tphB_{II}$-$tphA1_{II}$ (Fig. 2B). However, no product was observed when a primer pair that spans $tphR_{II}$-$tphC_{II}$ was used. These results suggest that all the tph_{II} catabolism genes except $tphR_{II}$ are organized in the same transcriptional unit, with $tphR_{II}$ being transcribed divergently from $tphC_{II}$.

Determination of transcription start site of tph_{II} catabolism operon. The transcription start site of the tph_{II} catabolism operon was determined by primer extension analysis using a primer, PEtphC110, that anneals to $tphC_{II}$ sequences. Due to the fact that no significant extension product was observed when total RNA from E6 cells was used as the template, total RNAs were prepared from E6 cells harboring plasmid pKTtphII, which carries $tphR_{II}C_{II}A2_{II}A3_{II}B_{II}A1_{II}$. In this analysis, a single major product was observed using RNA isolated from the cells grown in W minimal salt medium containing succinate and TPA (Fig. 3A), while no product was obtained with RNA isolated from the cells grown on succinate (data not shown). The transcription start site of the tph_{II} catabolism operon was mapped at the C residue located at 21 nucleotides upstream from the ATG start codon of $tphC_{II}$ (Fig. 3B). Putative −35 (TTAACA) and −10 (CATACT) sequences were found upstream of the transcription start site. We also carried out a primer extension analysis to determine the transcription start site of $tphR_{II}$; however, no extension product was obtained under our experimental conditions.

Promoter activities of tph_{II} catabolism operon and $tphR_{II}$. The $tphR_{II}$-$tphC_{II}$ intergenic region amplified by PCR was cloned into the promoter-probe vector pPR9TZ to generate a transcriptional fusion to the promoterless *lacZ* reporter gene. The resulting $tphC_{II}$ promoter-*lacZ* fusion plasmid, pZTC, included a DNA fragment which spans from positions −254 to +127 in relation to the transcription start site of $tphC_{II}$. The levels of expression of the $tphC_{II}$ promoter were examined in E6 and EME009 cells harboring pZTC. β-Galactosidase activity of E6 cells harboring pZTC was detected only in the cells grown in the presence of TPA (Table 3); therefore, the *cis*-acting region necessary for the transcriptional activation of the tph_{II} catabolism operon appeared to be in the $tphR_{II}$-$tphC_{II}$ intergenic region. $tphC_{II}$ promoter activity in response to TPA was also detected in EME009 cells harboring pZTC (Table 3), suggesting that the presence of $tphR_{II}$ is sufficient to control the inducible expression of the tph_{II} catabolism operon. In the cells of EME011 (Fig. 1B) harboring pZTC, which lacks the ability to transform TPA, $tphC_{II}$ promoter activity was observed by supplementation with TPA (Table 3). This result demonstrates that TPA itself acts as an inducer for the tph_{II} catabolism operon. In addition, the $tphC_{II}$ promoter activities observed in the presence of isophthalate, *o*-phthalate, or PCA were negligible; and these were also found in the absence of

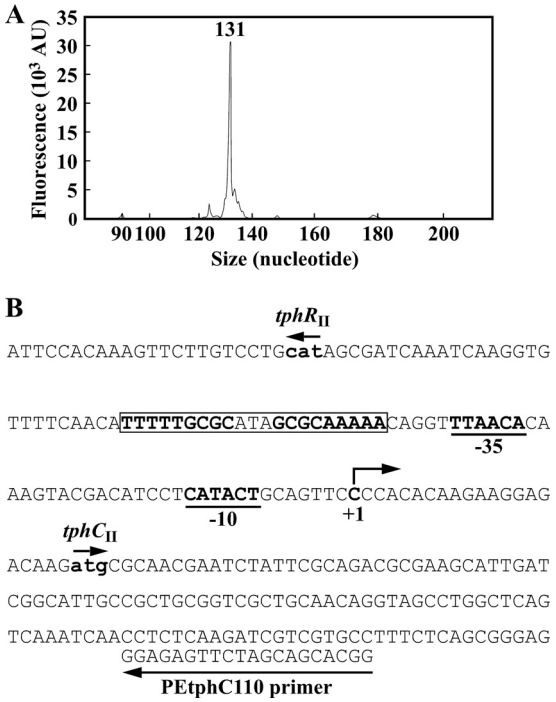

FIG. 3. Determination of the transcription start site of the $tphC_{II}$ operon. (A) Fluorescent primer extension was performed with D4-labeled primer PEtphC110 and 5 μg of total RNA isolated from E6 cells harboring pKTtphII grown in W minimal salt medium containing 10 mM succinate with 10 mM TPA. The transcription start site was determined by comparing the retention time of the D4-labeled primer extension product with the retention times of DNA size standards. AU, arbitrary fluorescence units. (B) Nucleotide sequence of the $tphR_{II}$-$tphC_{II}$ intergenic region. The initiation codons for $tphR_{II}$ and $tphC_{II}$ are indicated by boldface lowercase letters. The transcription start site (position +1), putative −10 and −35 regions of the $tphC_{II}$ promoter, and sequence of PEtphC110 are indicated. The inverted repeat sequence is boxed.

either compound (data not shown). The $tphR_{II}$ promoter activity was constitutively expressed at a low level in E6 and EME009 cells, both harboring the $tphR_{II}$ promoter-*lacZ* fusion plasmid pZTR (Table 3).

Disruption of $tphR_{II}$. The $tphR_{II}$ gene in EME009 was inactivated by the gene replacement technique with the $tphR_{II}$ disruption plasmid pDTRII so as to evaluate the role of $tphR_{II}$ in TPA catabolism. The ability of the resulting mutant, EME010 (Fig. 1B), to grow on TPA was completely lost (Fig. 4). To determine if this growth deficiency was caused by the disruption of $tphR_{II}$, pKTRII, which contains the 1.8-kb KpnI fragment carrying $tphR_{II}$ in pKT230MC, was introduced into EME010 cells. Complementation of EME010 with $tphR_{II}$ restored the growth of the mutant on TPA (Fig. 4). These results indicate that $tphR_{II}$ is essential for the TPA catabolism by EME009 cells.

TABLE 3. Promoter activities of $tphC_{II}$ and $tphR_{II}$

Promoter	Strain	β-Galactosidase activity (mU/mg)	
		With TPA	Without TPA
$tphC_{II}$ (pZTC)	E6	2.03 ± 0.14	ND[a]
	EME009	2.02 ± 0.12	ND
	EME011	2.53 ± 0.18	ND
	EME010	ND	ND
$tphR_{II}$ (pZTR)	E6	0.04 ± 0.01	0.04 ± 0.01
	EME009	0.05 ± 0.01	0.06 ± 0.01
	EME010	0.11 ± 0.02	0.09 ± 0.003

[a] ND, not detected.

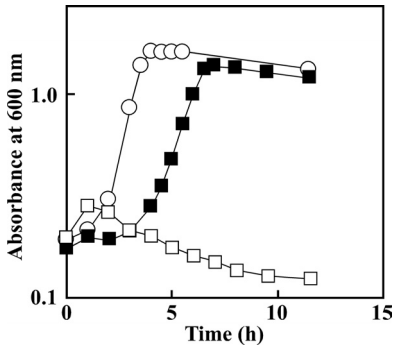

FIG. 4. Growth of E6 and EME010 cells on TPA. E6 (open circles), EME010 (open squares), and EME010 cells harboring pKTRII carrying $tphR_{II}$ (closed squares) were grown in W minimal salt medium containing 10 mM TPA. The results are the means of the representatives of three independent experiments. Error bars are hidden behind the symbols.

In order to confirm whether the $tphR_{II}$ gene product plays a role in the transcriptional regulation of the tph_{II} catabolism operon, the $tphC_{II}$ promoter activity in EME010 cells harboring pZTC was measured. When the cells were grown in the presence or absence of TPA, no activity was observed (Table 3), suggesting that $tphR_{II}$ encodes a transcriptional activator of the tph_{II} catabolism operon. On the other hand, the $tphR_{II}$ promoter activity of EME010 cells harboring pZTR was about 2.5-fold greater than that of cells of E6 and EME009 harboring the same plasmid (Table 3). $TphR_{II}$ appeared to negatively autoregulate the transcription from its own promoter, regardless of the presence of TPA, similar to that which was previously reported for ITTRs (24).

Binding of His-$TphR_{II}$ to the $tphR_{II}$-$tphC_{II}$ intergenic region. The His tag-fused $tphR_{II}$ gene was expressed in *E. coli* BL21(DE3) cells harboring pETtprII. Production of a 30-kDa protein in *E. coli* cells was observed by SDS-PAGE (data not shown). The size of this product was close to the predicted molecular mass of His-$TphR_{II}$ (M_r, 30,696). EMSAs were carried out using purified His-$TphR_{II}$ and the DIG-labeled RM149, RM102, RNM67, and RM31 probes covering nucleotide positions −103 to +46, −103 to −2, −21 to +46, and −66 to −36, respectively (position +1 is the $tphC_{II}$ transcription start site) (Fig. 5A). The binding experiments showed that the mobilities of the RM149, RM102, and RM31 fragments were retarded upon the addition of $TphR_{II}$, whereas no retardation was observed when the RNM67 probe was used (Fig. 5B). In these analyses, multiple complexes were observed. Because His-$TphR_{II}$ tended to aggregate during desalting, formation of multiple complexes might be related to the nature of His-$TphR_{II}$. The retardations were almost completely abolished when a 1,000-fold excess of the same unlabeled probe was added to the reaction mixtures. This confirmed that His-$TphR_{II}$ directly binds to the region from positions −66 to −36,

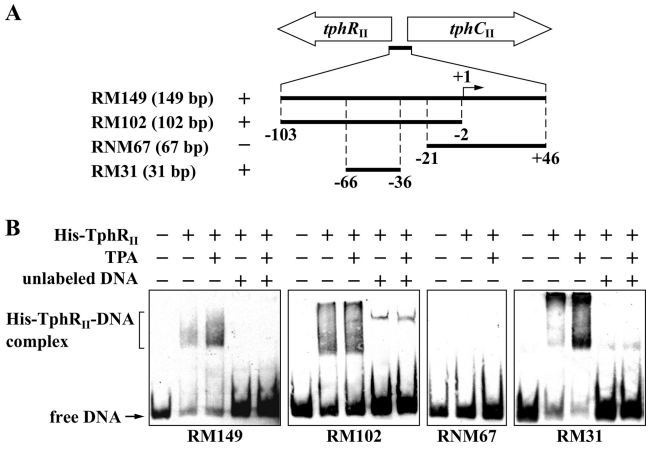

FIG. 5. Binding of His-TphR$_{II}$ to the *tphR*$_{II}$-*tphC*$_{II}$ intergenic region. (A) Schematic diagrams of the DNA fragments used in EMSAs. The sizes of the DNA probes are indicated in parentheses. The binding (+) and nonbinding (−) of the respective fragments are shown. The transcription start site (position +1) of *tphC*$_{II}$ is indicated. (B) EMSAs of the binding of purified His-TphR$_{II}$ to the *tphR*$_{II}$-*tphC*$_{II}$ intergenic region. The positions of the unbound probe (free DNA) and His-TphR$_{II}$-DNA complex are shown. His-TphR$_{II}$ (65 nM monomer), 100 μM TPA, and a 1,000-fold molar excess of the same unlabeled DNA fragment were added as indicated.

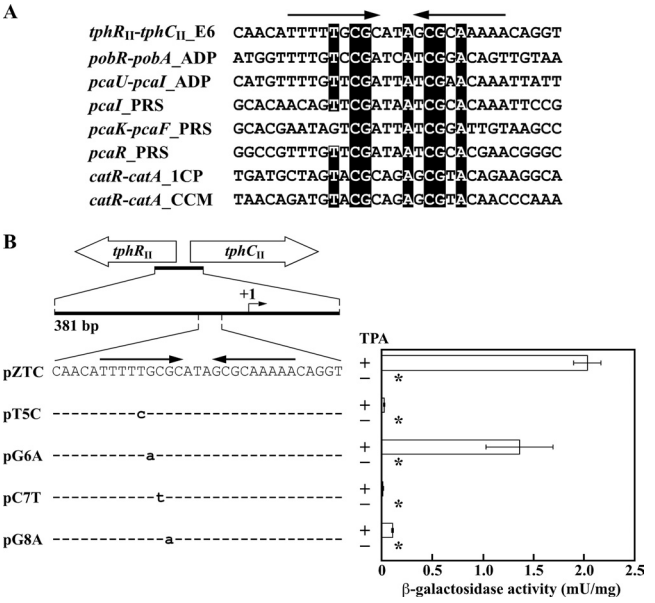

FIG. 6. β-Galactosidase activities from the wild-type and mutated *tphC*$_{II}$ promoters. (A) Alignment of the inverted repeat sequence of the *tphR*$_{II}$-*tphC*$_{II}$ intergenic region with the sequences involved in the binding of other ITTRs. Identical nucleotides are indicated by dark shading. The arrows indicate the inverted repeat sequence. Abbreviations (GenBank accession numbers): *tphR*$_{II}$-*tphC*$_{II}$_E6, the *tphR*$_{II}$-*tphC*$_{II}$ intergenic region of E6 (AB238679); *pobR-pobA*_ADP, the *pobR-pobA* intergenic region of *Acinetobacter baylyi* ADP1 (L05770); *pcaU-pcaI*_ADP, the *pcaU-pcaI* intergenic region of ADP1 (L05770); *pcaI*_PRS, the *pcaI* promoter region of *Pseudomonas putida* PRS2000 (M88763); *pcaK-pcaF*_PRS, the *pcaK-pcaF* intergenic region of PRS2000 (U10895); *pcaR*_PRS, the *pcaR* promoter region of PRS2000 (L33795); *catR-catA*_1CP, the *catR-catA* intergenic region of *Rhodococcus opacus* 1CP (X99622); *catR-catA*_CCM, the *catR-catA* intergenic region of *Rhodococcus erythropolis* CCM2595 (AJ605581). (B) Effect of mutations in the inverted repeat sequence on *tphC*$_{II}$ promoter activity. Mutated nucleotides are in lowercase. The arrows indicate the inverted repeat sequence. The transcription start site (position +1) of the *tphC*$_{II}$ promoter is indicated. E6 cells harboring each plasmid were grown in W minimal salt medium containing 10 mM succinate either with or without 10 mM TPA. Each value is the average ± standard deviation (error bars) based on at least three independent experiments. Asterisks, activities lower than the limit of detection.

which contains an inverted repeat sequence, 5′-TTTTTGCGCATAGCGCAAAAA-3′, centered at position −51 from the *tphC*$_{II}$ transcription start site. In the case of the binding sites for several ITTRs, including PcaU, PcaR, and PobR, an external direct sequence repetition of the half site of the inverted repeat sequences was observed (7, 11, 16, 28); and this direct sequence repetition was required for the binding of PcaU (28). No such direct repeat sequence was found in the *tphR*$_{II}$-*tphC*$_{II}$ intergenic region. In the case of other ITTRs, effector molecules had no effect on the affinity of the protein-DNA interactions (24). TPA also had no obvious effect on the binding of His-TphR$_{II}$ to the *tphR*$_{II}$-*tphC*$_{II}$ intergenic region.

Site-directed mutagenesis of the inverted repeat sequence. The existence of an inverted repeat sequence in the binding sites for PobR, PcaU, PcaR, and CatR has been reported (7, 10, 11, 36). Alignment of the inverted repeat sequences in the binding sites for TphR$_{II}$ and these ITTRs revealed that T, C, G, A, C, G, and A at positions −57, −55, −54, −50, −48, −47, and −45 from the *tphC*$_{II}$ transcriptional start site, respectively, are highly conserved (Fig. 6A). To investigate the involvement of these conserved nucleotides in the transcriptional activation from the *tphC*$_{II}$ promoter, conserved nucleotides T, C, and G, at positions −57, −55, and −54, respectively, were substituted by site-directed mutagenesis (Fig. 6B). The *tphC*$_{II}$ promoter activities of E6 cells harboring mutated *tphC*$_{II}$ promoter-*lacZ* fusion plasmid pT5C (T to C at position −57), pCT7 (C to T at position −55), or pG8A (G to A at position −54) and grown in the presence of TPA were only 0.9, 0.4, and 4.7%, respectively, of the activity obtained by E6 cells harboring pZTC grown under the same conditions. On the other hand, a single change from G at position −56, which is not conserved, to A (pG6A) resulted in only a slightly reduced β-galactosidase level (Fig. 6B). These results indicate that the T at residue −57, the C at residue −55, and the G at residue −54, which are conserved in the inverted repeat sequences, are important for TPA-dependent transcriptional activation from the *tphC*$_{II}$ promoter.

To investigate whether these nucleotides play a role in the formation of the His-TphR$_{II}$-DNA complex, EMSAs were performed with the mutated *tphC*$_{II}$ promoter probes (Fig. 7A). As shown in Fig. 7B, the C7T (C to T at position −55) probe was not bound by His-TphR$_{II}$, and significantly weak bindings were observed for the T5C (T to C at position −57) and G8A (G to A at position −54) probes. On the other hand, His-TphR$_{II}$ formed high-affinity complexes with the G6A (G to A at position −56) probe, similar to that which was found for the wild-type probe (Fig. 7B). These binding profiles correlated with the *tphC*$_{II}$ promoter activities. On the basis of these results, it is concluded that the conserved nucleotides are crucial for the ability to form the His-TphR$_{II}$-DNA complex. Furthermore, the binding of TphR$_{II}$ to the inverted repeat sequence is required for the inducible expression of the *tph*$_{II}$ catabolism

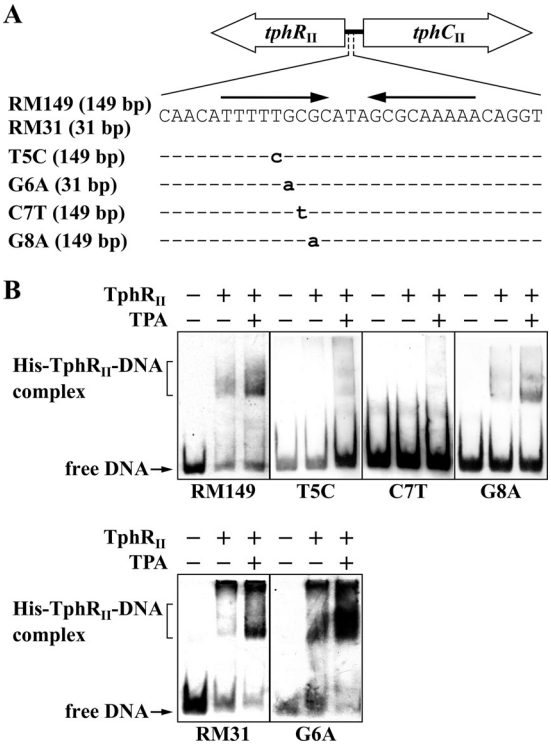

FIG. 7. EMSAs of the binding of His-TphR_{II} to the *tphC*$_{II}$ promoter regions containing mutated inverted repeat sequences. (A) Schematic diagrams of the DNA fragments used in EMSAs. Mutated nucleotides are in lowercase. The sizes of the DNA probes are indicated in parentheses. The arrows indicate the inverted repeat sequence. (B) EMSAs of the binding of purified His-TphR_{II} to the RM149 and RM31 probes and their mutant derivatives. The positions of the unbound probe (free DNA) and His-TphR_{II}-DNA complex are indicated. His-TphR_{II} (65 nM monomer) and 100 μM TPA were added as indicated.

operon in E6. The promoter region of the TPA catabolism gene cluster of *C. testosteroni* YZW-D (GenBank accession no. AY923836) showed 100% identity with the promoter regions of the *tph*$_{I/II}$ gene clusters, and the deduced amino acid sequences between E6 *tphR*$_{II}$ and YZW-D *tphR* showed 97% identity. These observations suggest that a common regulatory mechanism for the TPA catabolism genes exists in strains E6 and YZW-D.

Conclusions. The TPA-induced expression of the *tphC*$_{II}$*A2*$_{II}$*A3*$_{II}$*B*$_{II}$*A1*$_{II}$ operon of *Comamonas* sp. strain E6 is controlled by TphR_{II}, which belongs to the ITTR family. His-TphR_{II} specifically binds to the inverted repeat sequence within the *tphC*$_{II}$-*tphR*$_{II}$ intergenic region. The nucleotides in the inverted repeat sequences highly conserved among the promoter regions, which interact with PcaU, PcaR, PobR, and CatR, are essential for the TPA-dependent transcriptional activation from the *tphC*$_{II}$ promoter and the formation of the His-TphR_{II}-DNA complex.

REFERENCES

1. **Abe, T., E. Masai, K. Miyauchi, Y. Katayama, and M. Fukuda.** 2005. A tetrahydrofolate-dependent *O*-demethylase, LigM, is crucial for catabolism of vanillate and syringate in *Sphingomonas paucimobilis* SYK-6. J. Bacteriol. **187:**2030–2037.
2. **Blatny, J. M., T. Brautaset, H. C. Winther-Larsen, P. Karunakaran, and S. Valla.** 1997. Improved broad-host-range RK2 vectors useful for high and low regulated gene expression levels in Gram-negative bacteria. Plasmid **38:**35–51.
3. **Bradford, M. M.** 1976. A rapid and sensitive method for the quantitation of microgram quantities of protein utilizing the principle of protein-dye binding. Anal. Biochem. **72:**248–254.
4. **Choi, K. Y., D. Kim, W. J. Sul, J. C. Chae, G. J. Zylstra, Y. M. Kim, and E. Kim.** 2005. Molecular and biochemical analysis of phthalate and terephthalate degradation by *Rhodococcus* sp. strain DK17. FEMS Microbiol. Lett. **252:**207–213.
5. **Dal, S., G. Trautwein, and U. Gerischer.** 2005. Transcriptional organization of genes for protocatechuate and quinate degradation from *Acinetobacter* sp. strain ADP1. Appl. Environ. Microbiol. **71:**1025–1034.
6. **DiMarco, A. A., B. Averhoff, and L. N. Ornston.** 1993. Identification of the transcriptional activator *pobR* and characterization of its role in the expression of *pobA*, the structural gene for *p*-hydroxybenzoate hydroxylase in *Acinetobacter calcoaceticus*. J. Bacteriol. **175:**4499–4506.
7. **DiMarco, A. A., and L. N. Ornston.** 1994. Regulation of *p*-hydroxybenzoate hydroxylase synthesis by PobR bound to an operator in *Acinetobacter calcoaceticus*. J. Bacteriol. **176:**4277–4284.
8. **Eaton, R. W.** 2001. Plasmid-encoded phthalate catabolic pathway in *Arthrobacter keyseri* 12B. J. Bacteriol. **183:**3689–3703.
9. **Fukuhara, Y., K. Inakazu, N. Kodama, N. Kamimura, D. Kasai, Y. Katayama, M. Fukuda, and E. Masai.** 2010. Characterization of the isophthalate degradation genes of *Comamonas* sp. strain E6. Appl. Environ. Microbiol. **76:**519–527.
10. **Gerischer, U., A. Segura, and L. N. Ornston.** 1998. PcaU, a transcriptional activator of genes for protocatechuate utilization in *Acinetobacter*. J. Bacteriol. **180:**1512–1524.
11. **Guo, Z., and J. E. Houghton.** 1999. PcaR-mediated activation and repression of *pca* genes from *Pseudomonas putida* are propagated by its binding to both the −35 and the −10 promoter elements. Mol. Microbiol. **32:**253–263.
12. **Hanahan, D.** 1983. Studies on transformation of *Escherichia coli* with plasmids. J. Mol. Biol. **166:**557–580.
13. **Hara, H., L. D. Eltis, J. E. Davies, and W. W. Mohn.** 2007. Transcriptomic analysis reveals a bifurcated terephthalate degradation pathway in *Rhodococcus* sp. strain RHA1. J. Bacteriol. **189:**1641–1647.
14. **Harwood, C. S., and R. E. Parales.** 1996. The β-ketoadipate pathway and the biology of self-identity. Annu. Rev. Microbiol. **50:**553–590.
15. **Hishida, M., K. Shikinaka, Y. Katayama, S. Kajlta, E. Masai, M. Nakamura, Y. Otsuka, S. Ohara, and K. Shigehara.** 2009. Polyesters of 2-pyrone-4,6-dicarboxylic acid (PDC) as bio-based plastics exhibiting strong adhering properties. Polym. J. **41:**297–302.
16. **Jerg, B., and U. Gerischer.** 2008. Relevance of nucleotides of the PcaU binding site from *Acinetobacter baylyi*. Microbiology **154:**756–766.
17. **Kasai, D., T. Fujinami, T. Abe, K. Mase, Y. Katayama, M. Fukuda, and E. Masai.** 2009. Uncovering the protocatechuate 2,3-cleavage pathway genes. J. Bacteriol. **191:**6758–6768.
18. **Kasai, D., E. Masai, K. Miyauchi, Y. Katayama, and M. Fukuda.** 2005. Characterization of the gallate dioxygenase gene: three distinct ring cleavage dioxygenases are involved in syringate degradation by *Sphingomonas paucimobilis* SYK-6. J. Bacteriol. **187:**5067–5074.
19. **Kersten, P. J., S. Dagley, J. W. Whittaker, D. M. Arciero, and J. D. Lipscomb.** 1982. 2-Pyrone-4,6-dicarboxylic acid, a catabolite of gallic acids in *Pseudomonas* species. J. Bacteriol. **152:**1154–1162.
20. **Masai, E., Y. Katayama, and M. Fukuda.** 2007. Genetic and biochemical investigations on bacterial catabolic pathways for lignin-derived aromatic compounds. Biosci. Biotechnol. Biochem. **71:**1–15.
21. **Masai, E., S. Shinohara, H. Hara, S. Nishikawa, Y. Katayama, and M. Fukuda.** 1999. Genetic and biochemical characterization of a 2-pyrone-4,6-dicarboxylic acid hydrolase involved in the protocatechuate 4,5-cleavage pathway of *Sphingomonas paucimobilis* SYK-6. J. Bacteriol. **181:**55–62.
22. **Michinobu, T., M. Bito, M. Tanimura, Y. Katayama, E. Masai, M. Nakamura, Y. Otsuka, S. Ohara, and K. Shigehara.** 2009. Mechanical properties of poly(L-lactide) films controlled by blending with polyesters of lignin-derived stable metabolic intermediate, 2-pyrone-4,6-dicarboxylic acid (PDC). Polym. J. **41:**843–848.
23. **Michinobu, T., M. Hishida, M. Sato, Y. Katayama, E. Masai, M. Nakamura, Y. Otsuka, S. Ohara, and K. Shigehara.** 2008. Polyesters of 2-pyrone-4,6-dicarboxylic acid (PDC) obtained from a metabolic intermediate of lignin. Polym. J. **40:**68–75.
24. **Molina-Henares, A. J., T. Krell, M. Eugenia Guazzaroni, A. Segura, and J. L. Ramos.** 2006. Members of the IclR family of bacterial transcriptional regulators function as activators and/or repressors. FEMS Microbiol. Rev. **30:**157–186.
25. **Nishikawa, S., T. Sonoki, T. Kasahara, T. Obi, S. Kubota, S. Kawai, N. Morohoshi, and Y. Katayama.** 1998. Cloning and sequencing of the *Sphingomonas* (*Pseudomonas*) *paucimobilis* gene essential for the O demethylation of vanillate and syringate. Appl. Environ. Microbiol. **64:**836–842.
26. **Patrauchan, M. A., C. Florizone, M. Dosanjh, W. W. Mohn, J. Davies, and L. D. Eltis.** 2005. Catabolism of benzoate and phthalate in *Rhodococcus* sp. strain RHA1: redundancies and convergence. J. Bacteriol. **187:**4050–4063.
27. **Peng, X., T. Egashira, K. Hanashiro, E. Masai, S. Nishikawa, Y. Katayama,**

K. Kimbara, and M. Fukuda. 1998. Cloning of a *Sphingomonas paucimobilis* SYK-6 gene encoding a novel oxygenase that cleaves lignin-related biphenyl and characterization of the enzyme. Appl. Environ. Microbiol. **64:**2520–2527.
28. **Popp, R., T. Kohl, P. Patz, G. Trautwein, and U. Gerischer.** 2002. Differential DNA binding of transcriptional regulator PcaU from *Acinetobacter* sp. strain ADP1. J. Bacteriol. **184:**1988–1997.
29. **Romero-Steiner, S., R. E. Parales, C. S. Harwood, and J. E. Houghton.** 1994. Characterization of the *pcaR* regulatory gene from *Pseudomonas putida*, which is required for the complete degradation of *p*-hydroxybenzoate. J. Bacteriol. **176:**5771–5779.
30. **Sasoh, M., E. Masai, S. Ishibashi, H. Hara, N. Kamimura, K. Miyauchi, and M. Fukuda.** 2006. Characterization of the terephthalate degradation genes of *Comamonas* sp. strain E6. Appl. Environ. Microbiol. **72:**1825–1832.
31. **Schäfer, A., A. Tauch, W. J. Jäger, J. Kalinowski, G. Thierbach, and A. Pühler.** 1994. Small mobilizable multi-purpose cloning vectors derived from the *Escherichia coli* plasmids pK18 and pK19: selection of defined deletions in the chromosome of *Corynebacterium glutamicum*. Gene **145:**69–73.
32. **Schläfli, H. R., M. A. Weiss, T. Leisinger, and A. M. Cook.** 1994. Terephthalate 1,2-dioxygenase system from *Comamonas testosteroni* T-2: purification and some properties of the oxygenase component. J. Bacteriol. **176:**6644–6652.
33. **Shigematsu, T., K. Yumihara, Y. Ueda, S. Morimura, and K. Kida.** 2003. Purification and gene cloning of the oxygenase component of the terephthalate 1,2-dioxygenase system from *Delftia tsuruhatensis* strain T7. FEMS Microbiol. Lett. **220:**255–260.
34. **Short, J. M., J. M. Fernandez, J. A. Sorge, and W. D. Huse.** 1988. λ ZAP: a bacteriophage λ expression vector with *in vivo* excision properties. Nucleic Acids Res. **16:**7583–7600.
35. **Studier, F. W., and B. A. Moffatt.** 1986. Use of bacteriophage T7 RNA polymerase to direct selective high-level expression of cloned genes. J. Mol. Biol. **189:**113–130.
36. **Veselý, M., M. Knoppová, J. Nešvera, and M. Pátek.** 2007. Analysis of *catRABC* operon for catechol degradation from phenol-degrading *Rhodococcus erythropolis*. Appl. Microbiol. Biotechnol. **76:**159–168.
37. **Wang, Y. Z., Y. Zhou, and G. J. Zylstra.** 1995. Molecular analysis of isophthalate and terephthalate degradation by *Comamonas testosteroni* YZW-D. Environ. Health Perspect. **103**(Suppl. 5)**:**9–12.